ELSEVIER

Chemical Engineering Journal 133 (2007) 139–149

Chemical Engineering Journal

www.elsevier.com/locate/cej

Prediction of regime transitions in bubble columns using acoustic and differential pressure signals

Waheed A. Al-Masry *, Emad M. Ali, Mohamed N. Al-Kalbani

Department of Chemical Engineering, King Saud University, Riyadh, Saudi Arabia

Received 15 July 2006; received in revised form 13 February 2007; accepted 20 February 2007

Abstract

This paper addresses the identification of the transition points of the flow regimes in bubble columns. For this purpose, statistical and spectral analysis of the acoustic sound signals and differential pressure signals were employed over several values of the gas velocity. Both analysis tools were able to extract useful qualitative and quantitative information about the flow patterns. In addition, applying the two methods to both types of signals presented comparable results about the quantitative values of the critical velocities. These values agree well with those reported in the literature. Moreover, the implementation of the auto-correlation function on the differential pressure signal was found helpful in determining period of the macro-structure fluctuation.

Keywords: Differential pressure; Bubble column; Hydrodynamics; Regime transition; Time series analysis

1. Introduction

Bubble columns are multiphase reactors that are widely used in the chemical and petrochemical industries. The success of bubble columns is attributed to the advantages they offer over the other kind of multiphase reactors. For example, they have simple construction, minimum mechanically vibrating parts, good heat and mass transfer properties, good mixing, low power requirements and high thermal stability [1]. Bubble columns are known to have complex hydrodynamic properties. Up to this point, it is found that two hydrodynamic flow patterns exist in these columns. First of which is the homogeneous regime which occurs at low gas velocity followed by a transition region and then the heterogeneous regime which occurs at high gas velocities [2]. The transition could be instantaneous and hence represented by a single point, or expanded transition represented by two points, i.e., beginning and end. The bubble properties (such as bubble size, shape and velocity) play an important role in the column hydrodynamics. Other factors that influence the hydrodynamics of the column are the column geometry, sparger design, operating conditions, and physico-chemical properties of the gas–liquid phases. The variation of those parameters strongly affects the two flow regimes making the hydrodynamics more complicated. Consequently, further research and analysis to deeply understand the hydrodynamic behavior of bubble columns and its sources will enhance its operation, design and scale-up. For this reason, several techniques to measure the bubble size, shape and velocity were developed and tested. A review of these methods can be found elsewhere [3].

Recently most of the work dealing with studying the bubble properties and/or flow transitions is centered on the measurement of gas holdup, pressure fluctuation and acoustic sound [4–10]. Several types of analysis tools were successfully applied to extract useful information from the previously mentioned measurements. Among these tools are statistical [8,11,14], spectral [8,11,14], fractal [8,12], time series [8,9] and deterministic chaos [4,8]. Al-Masry et al. [3] have employed the spectral analysis to acoustic sound measurements in air–water system to determine the bubble characteristics such as the bubble size, bubble distribution, damping factor of the bubble oscillation. Al-Masry et al. [5] and Al-Masry and Ali [13] have extended the work to include the addition of coalescence and non-coalescence agents to air–water system. The influence of such surfactant compounds on the overall bubble characteristics was investigated. It is found that acoustic measurements and spectral tools are helpful to unfold valuable information about the bubble properties especially the bubble size and its frequency of oscillation.

* Corresponding author.
E-mail address: walmasry@ksu.edu.sa (W.A. Al-Masry).

1385-8947/$ – see front matter © 2007 Elsevier B.V. All rights reserved.
doi:10.1016/j.cej.2007.02.025

Nomenclature

f	frequency (Hz)
n	number of detected peaks
N	number of data points
U_G	superficial gas velocity (m/s)
x	time series signal

Greek letter

σ	standard deviation

According to the various investigations mentioned above, the pressure fluctuation inside bubble columns has attracted a lot of attention. Unlike, the gas holdup measurement, the pressure signals can provide more local (detailed) information. In fact, pressure fluctuation signals found to be strongly related to the gas holdup and liquid-phase circulation. Consequently pressure fluctuation and/or differential pressure measurements were used to identify the flow regimes and transition points in bubble columns [12,1]. Another attractive point is that such pressure transducers are commonly utilized in process industries because it is robust, cheap and well developed. A major difference between the pressure signals and acoustic signals is that the former is not used to infer information about the bubble size.

As mentioned earlier, bubble columns are known to have two transition points that distinguish two flow patterns. The first flow pattern is the homogeneous regime or bubble flow, and the second pattern is the heterogeneous or turbulent flow. The aim of this paper is thus to investigate the capability of acoustic sound signals to identify the flow regimes. In fact, the standard deviation and spectral density of the bubble sound measurements will be used for this purpose. Moreover, differential pressure signals will be also exploited to confirm and/or complement the results found from the acoustic signals. In this regard, statistical, spectral and auto-correlation analysis will be applied.

2. Equipment and experimental methods

Schematic diagram of the experimental setup is shown in Fig. 1. Details of the experimental setup, acoustic measurement techniques and analysis can be found elsewhere [3,5,13]. The column is made from Perspex with 0.15 m in diameter and 0.7 m in clear liquid height. The gas distributor is made from brass was a six legs star like cross, with 85 holes and 1 mm diameter equally distributed. Air from cylinder was used as the sparging gas with superficial gas velocity up to 0.1 m/s, and liquid was tap water supplied from university supply system. In this work, pressure fluctuations were measured using two different techniques: form inside the column using miniature hydrophone, and from outside the column using differential pressure meter between two points at the column wall. The hydrophone (Bruel & Kjær type 8103, Denmark) signals were pre-amplified by Bruel & Kjær type 2635 charge amplifier, and set to the given calibration.

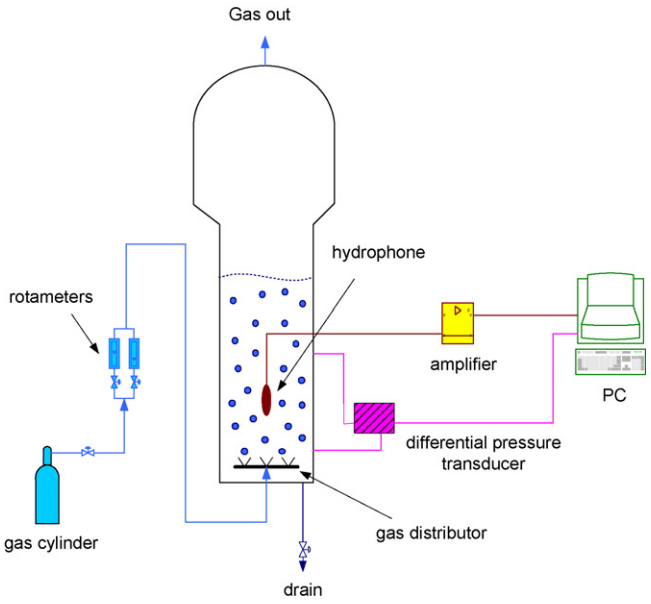

Fig. 1. Schematic diagram of the experimental setup.

Acoustic pressures were digitized as voltage signals using Data Translation (USA) data acquisition system. Pressure changes between two points at the column wall were monitored using Omega 205-2 differential pressure meter (USA), and digitized using Data Translation DT9805 board (USA) and captured by Data Translation Measure Foundry software (USA).

3. Results and discussion

It is well known that the hydrodynamics of bubble columns can be described by two distinguished flow patterns. The first flow pattern is the homogeneous regime which occurs at very low gas velocity and is characterized by uniform bubble-size distribution. The coalescence and breakup of bubbles as well as liquid-phase circulation are negligible. As the gas velocity increases the system undergoes a transition state where larger bubble formation and liquid-phase circulation starts. At high gas velocity, the liquid circulation becomes violent and larger bubble sizes are produced due to coalescence. At this stage, the homogeneous regime cannot be maintained and thus wide bubble-size distribution is observed, i.e., the flow regime is heterogeneous. This phenomenon is observed by many researchers using wall pressure and differential pressure fluctuation [4,6,7,11,14]. Statistical and spectral tools were applied to pressure signals. Negative peaks (valleys) or sudden changes in the statistical and/or spectrum trends are believed to indicate regime transition. Following the same approach, our results that are based on acoustic signals and pressure fluctuations agree well with the reported observations as discussed in the following sections.

3.1. Acoustic sound signals

Acoustic signals were measured over 2 s capture time and 20 kHz sampling frequency. The collected acoustic signal for

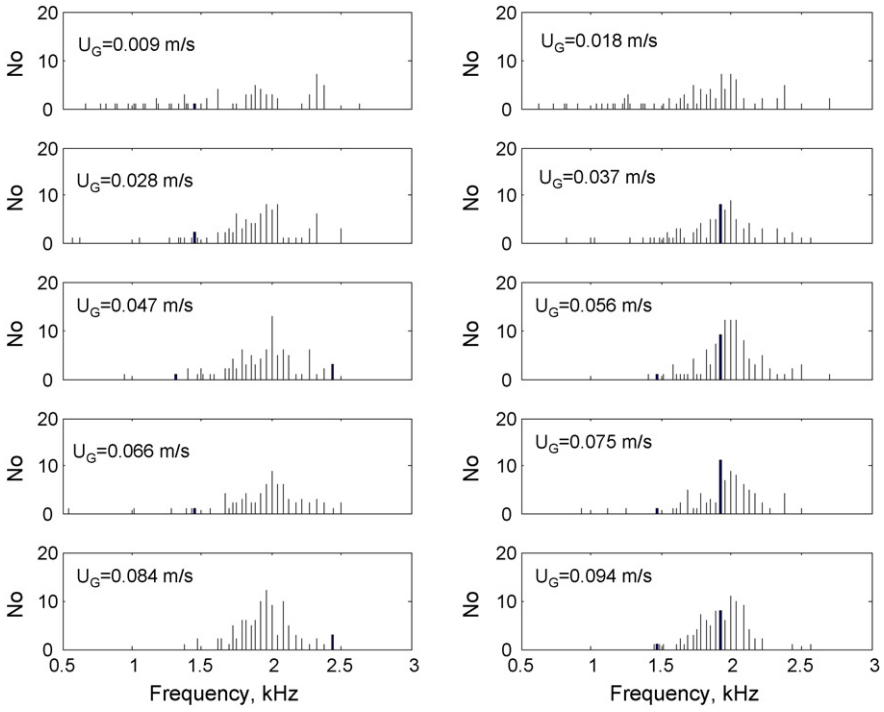

Fig. 2. Bubble frequency distribution of acoustic sound signals.

air–water system is filtered and transformed into spectrum as shown in Fig. 2 for various gas velocities. The result shown in Fig. 2 is reproduced from earlier work [3,5]. Note that the spectral transformation is applied to selected segments of the acoustic signal. The data segments are selected by our method of pulsation detection and triggering [3,5]. The spectrum in Fig. 2 represents the bubble frequency distribution, i.e., each column indicates a detected bubble pulsation with x-axes determine its frequency, f and the y-axes determine its intensity or number of occurrence, n. Note that the bubble diameter is inversely proportional to the pulsation frequency [3]. Investigating the spectrum for transition behavior is somewhat tricky. Therefore, we compute the average pulsation frequency using the following rule:

$$f_m = \frac{\sum_{i=1}^{nc} f_i n(f_i)}{\sum_{i=1}^{nc} n(f_i)} \quad (1)$$

Applying the above rule produces the average pulsation frequency shown in Fig. 3. Although the range of bubble frequency is narrow, the trend for air–water system shows the existence of two negative peaks at 0.037 and 0.066 m/s which represent the critical velocities at the transition points. These values agree well with the reported values in the literature as well as with the values obtained from pressure fluctuation as will be discussed later in the paper. The trend of average frequency shown in Fig. 3 indicates that the bubble size is slightly larger at lower gas velocity. This can be attributed to the sparger design as the distributor effect is more pronounced at low gas velocity than at high gas velocities [13]. When 0.05 wt% KCl is added to water, which acts as coalescence inhibitor, the frequency distribution grows gradually and then drop suddenly at 0.066 m/s. Apparently, only one critical velocity is still apparent and occurs at the same locations of the second transition point detected for air–water system. It is expected that the critical velocities be delayed for KCl solution because the surfactant media reduces the coalescence behavior causing prolonged homogeneous regime. Therefore, the single critical value could represent a lagged first transition point, i.e., end of homogeneous regime.

The evolution of the standard deviation of the acoustic signal is illustrated in Fig. 4. As mentioned earlier, as gas velocity increases the number of flowing bubbles and therefore their sound increase. Thus, the acoustic signal and consequently its σ intensify with increasing gas flow. In this case, standard deviation may not provide interesting information about the regime transitions (Letzel et al. [11]) or at the best it can only identify the end of the homogeneous regime [8]. Interestingly, Fig. 4 shows that for water system two transition points occur at 0.044 and

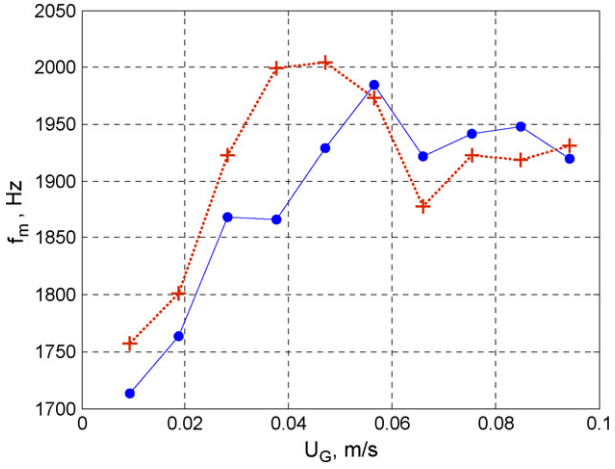

Fig. 3. Average bubble frequency; (solid): water and (dash): 0.05% KCl.

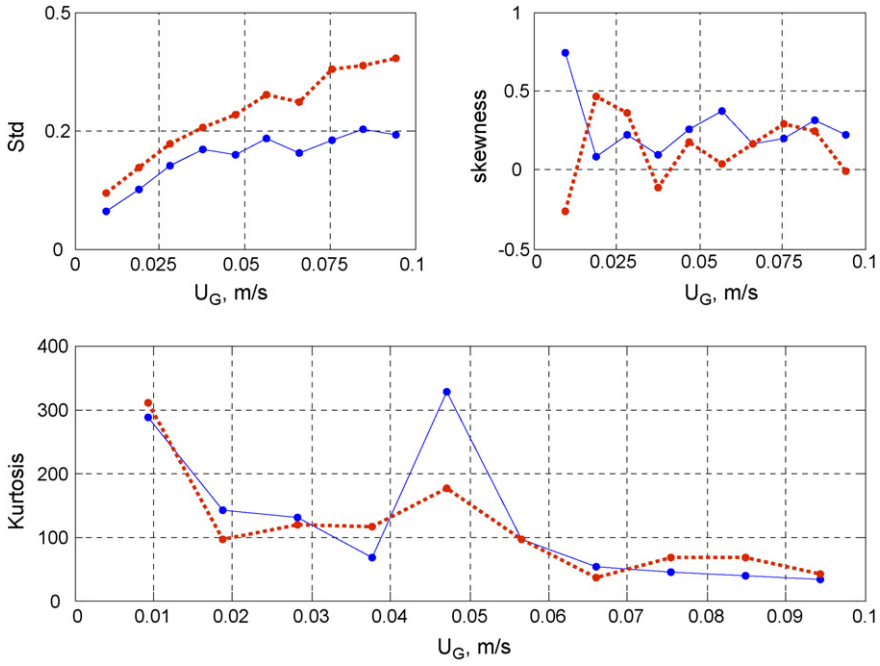

Fig. 4. Statistical moments of the acoustic sound signal; (solid): water and (dash): 0.05% KCl.

0.066 m/s. On the other hand, in the presence of tension-active agent a single critical value is obtained. This value could mark the end of lagged homogeneous regime or the beginning of a fully established regime.

The third and fourth moments of the probability distribution (skewness and kurtosis) are used to analyze the pressure signals. In probability theory and statistics, *skewness* is a measure of the asymmetry of the probability distribution of a real-valued random variable. Roughly speaking, a distribution has positive skew (right-skewed) if the right (higher value) tail is longer and negative skew (left-skewed) if the left (lower value) tail is longer. Skewness can be calculated from the following relation:

$$\text{skewness} = \frac{n}{(n-1)(n-2)} \sum_{i=1}^{n} \left(\frac{x_i - \bar{x}}{\sigma} \right)^3 \tag{2}$$

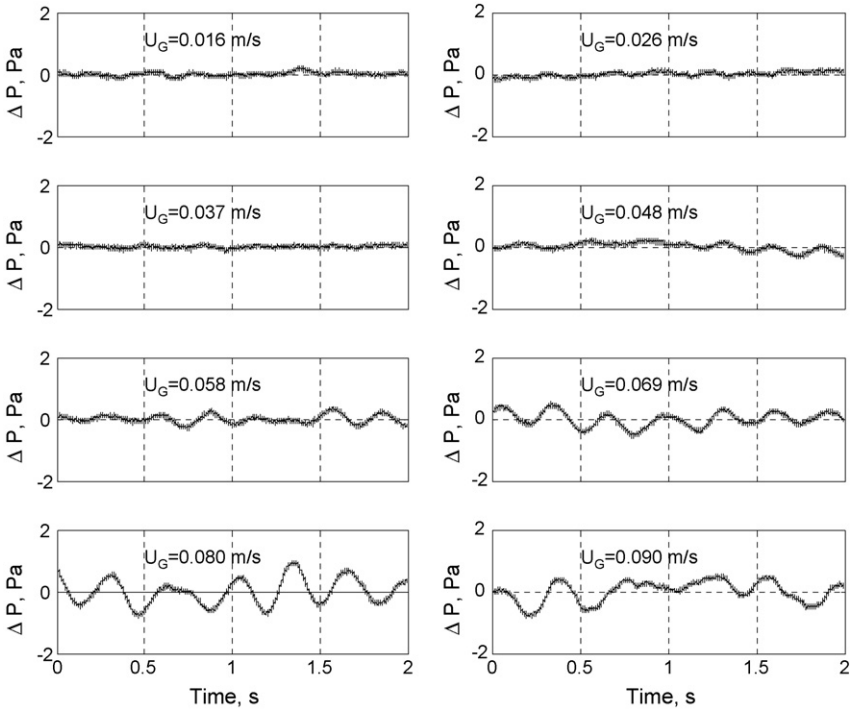

Fig. 5. Measured differential pressure fluctuation for air–water system.

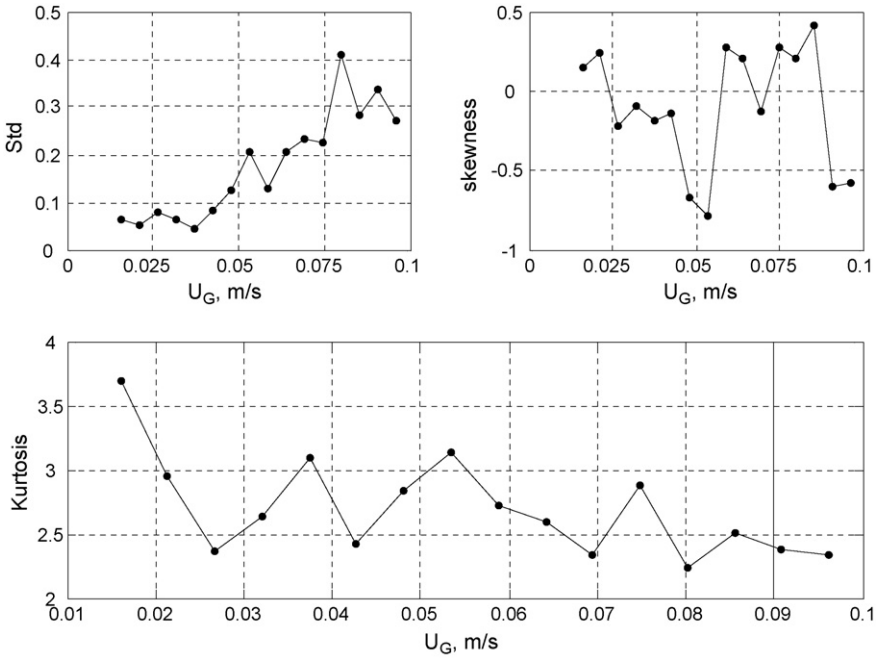

Fig. 6. Statistical moments of the differential pressure signal.

On the other hand, *kurtosis* is a measure of the "peakedness" of the probability distribution of a real-valued random variable. A high kurtosis distribution has a sharper peak and fatter tails, while a low kurtosis distribution has a more rounded peak and wider shoulders. The mathematical definition of kurtosis is given as follows:

$$\text{kurtosis} = \frac{n(n-1)}{(n-1)(n-2)(n-2)} \sum_{i=1}^{n} \left(\frac{x_i - \bar{x}}{\sigma} \right)^4 \times \frac{3(n-1)^2}{(n+2)(n+3)} \tag{3}$$

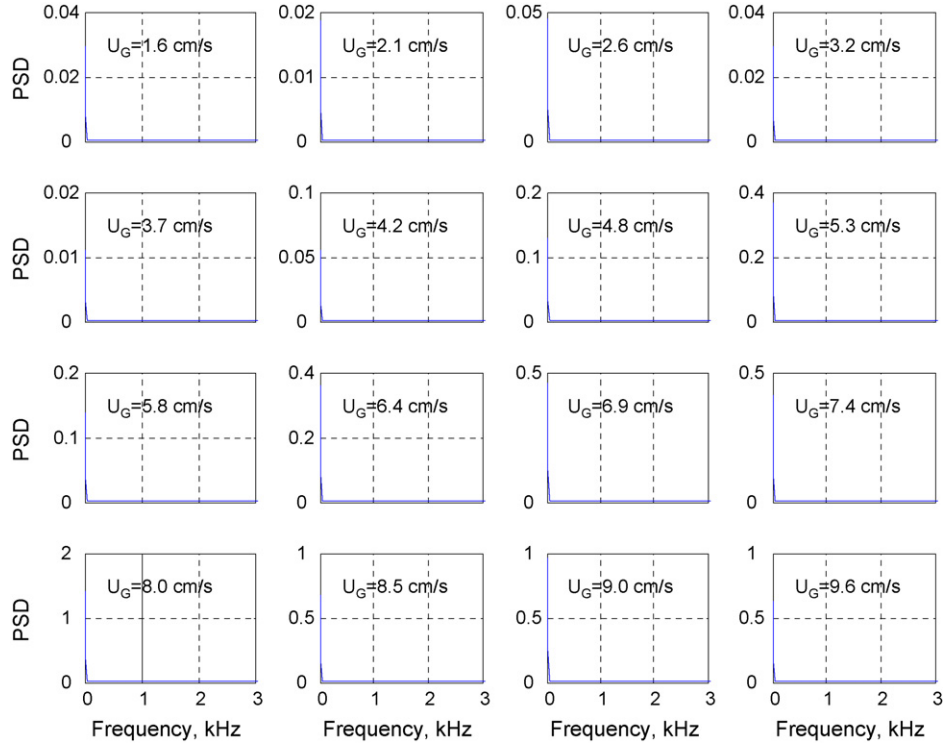

Fig. 7. Power spectrum density of the differential pressure using the full data record.

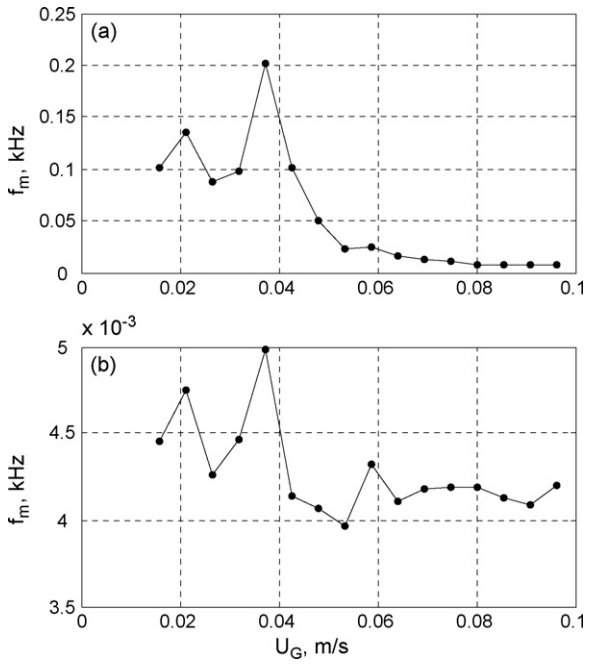

Fig. 8. Average frequency of the spectral density in Fig. 7; (a) high band and (b) low band.

Skewness was used by Vial et al. [8] and found not to provide any useful information while Kurtosis was able to reveal some related observations. Fig. 4 illustrates the variation of skewness and kurtosis for water and 0.05 wt% KCl solutions. As reported in the literature, skewness does not provide significant information except that for KCl solution the distribution move from positive skew to negative skew at 0.044 m/s. The latter is believed to be the critical value for the end of homogeneous regime. Similarly, the kurtosis distribution shows an apparent peak at 0.044 m/s for both air–water system and 0.05% KCl solution. Vial et al. [9] have reported that kurtosis exhibits a pronounced maximum when the holdup versus gas velocity trend passes through a maximum.

It should be noted that the high order moments are known to be less robust than the low order moments such as mean and variance. Moreover, the accuracy of the moment analysis is in general influenced by the size of the vessel, the position and the type of sensor. As a conclusion, it is shown that applying the spectral analysis to the acoustic sound signal is effective in analyzing the regime transition points. The finding also somewhat confirms those obtained from standard deviation and to some extent those obtained from high order moments. It follows that the acoustic sound measurements by hydrophone is not only effective for prediction of the bubble size and bubble-size distribution but also for identification of regime transition points.

3.2. Differential pressure signals

The raw signal of the differential pressure is depicted in Fig. 5. The pressure signal is sampled at 10 kHz frequency over a period of 2 s. Large sampling frequency is used to capture the high-frequency components. Short length of data record, e.g. 2 s, is used to avoid the very low-frequency oscillation, i.e., $f < 0.5$ Hz, caused by level dispersion. The pressure trends are mean removed for fair comparison. It is evident that at low gas velocity, the trend is almost steady because the flow is dominated by the bubble movements. Around gas velocity of

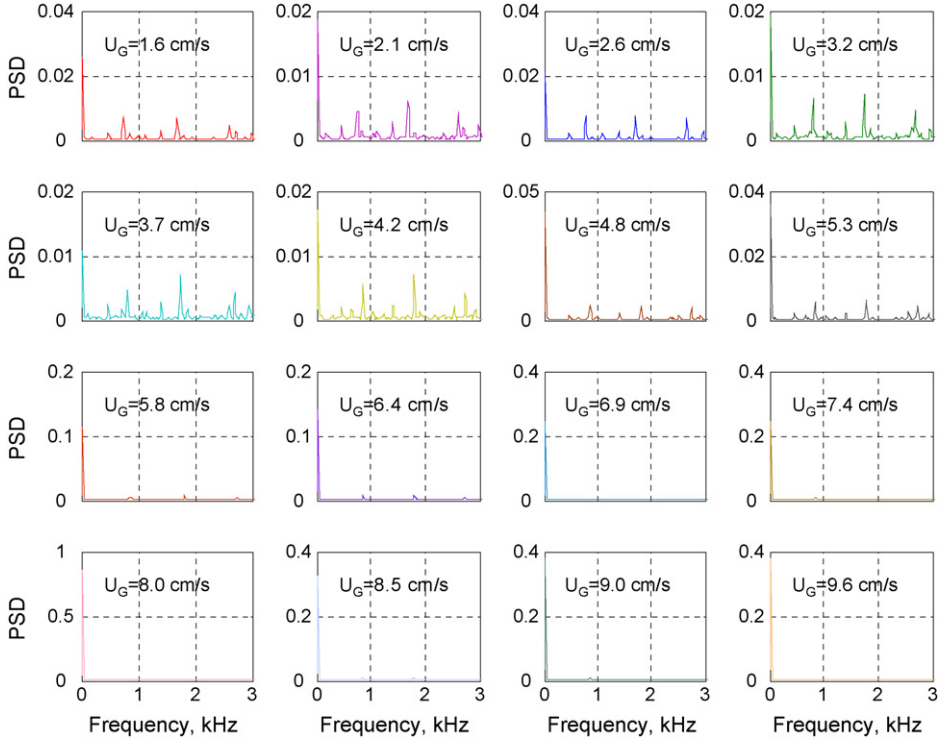

Fig. 9. Power spectrum density of the differential pressure using the average of several short segments.

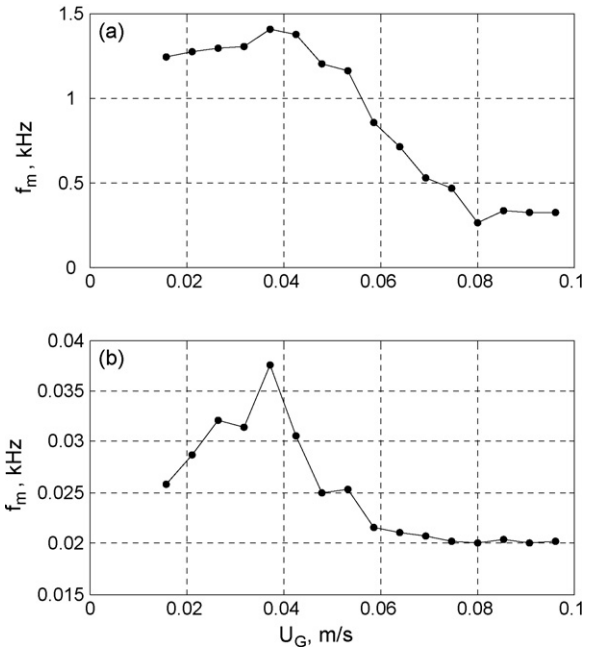

Fig. 10. Average frequency of the spectral density in Fig. 9; (a) high band and (b) low band.

0.058 m/s pressure fluctuation characterized by low frequency starts appearing. The pressure fluctuation becomes clearer as gas velocity propagates because of well-established liquid circulation. This circulation is reported [13] to have a frequency of 3–5 Hz and is induced by bubble to form macro-structures in the liquid phase. This behavior is in agreement with the hydrodynamic behavior discussed before. Visual inspection of the raw data reveals also the existence of high-frequency components. For further investigation we perform statistical and spectral analysis of the pressure fluctuation.

3.2.1. Statistical analysis

The second, third and fourth moments of the differential pressure is demonstrated in Fig. 6. It is expected that the deviation of the pressure signal from its mean will increase as gas flow increase because of growing fluid circulation and bubble-induced level fluctuation. Therefore, the standard deviation is expected to increase monotonically. However, a sudden drop in σ is observed at 0.037 m/s and another at 0.058 m/s. This variation in the data structure could be the result of a change in the flow behavior. These values coincide with the critical velocities found earlier. Moreover, It is clear from Fig. 5 that the pressure starts fluctuating at the value of 0.058 m/s for the gas velocity. Gourich et al. [1] have shown that for air–water system, the standard deviation for differential pressure is constant at velocity below 0.04 m/s, gradually increasing between 0.04 and 0.07 m/s and then remain constant above 0.07 m/s. They concluded that σ increase rapidly in the transition region and slowly in the heterogeneous regime. Our standard deviation for differential pressure shown in Fig. 6 delivered somewhat the same performance.

Skewness, on the other hand, maintain a negative value between 0.027 and 0.053 m/s and almost a positive value afterward except at very high gas flow. Interestingly, a pronounced change from negative to positive skew value occur between 0.053 and 0.058 m/s which complements the result obtained from the raw data and standard deviation. Conversely, the

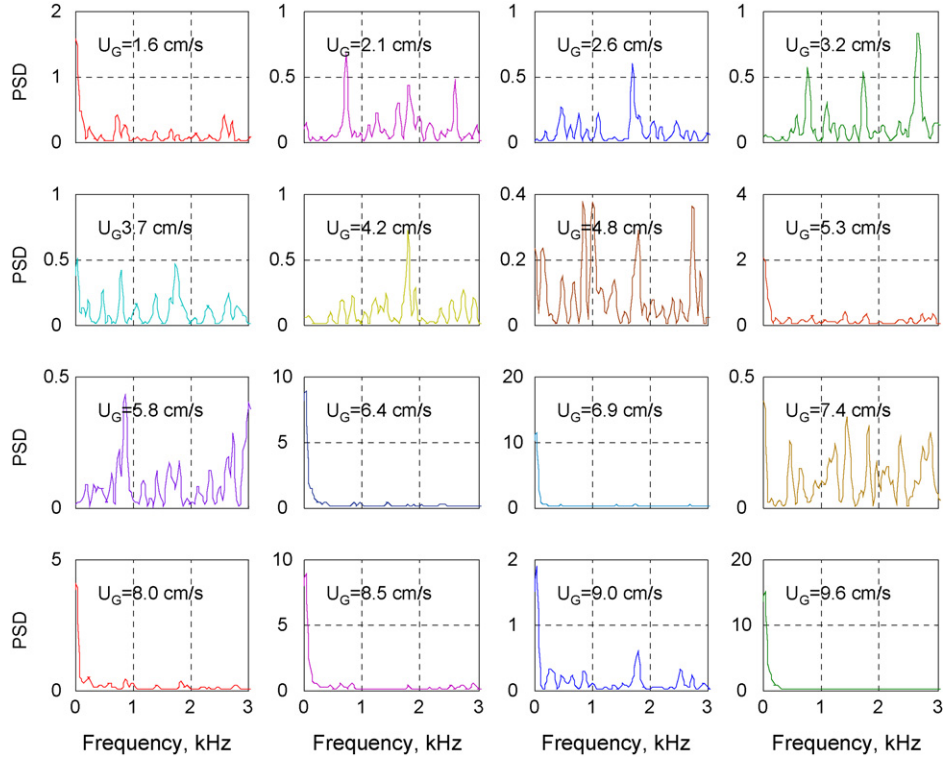

Fig. 11. Power spectrum density of the differential pressure using a short segment of the data record.

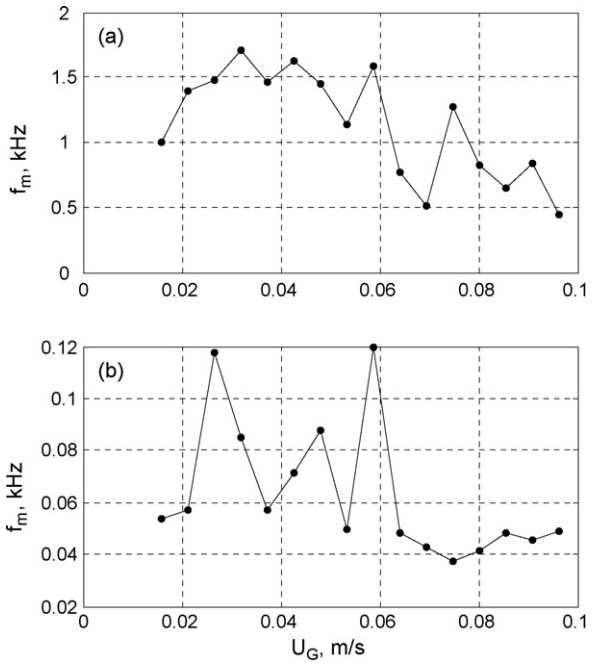

Fig. 12. Average frequency of the spectral density in Fig. 11; (a) high band and (b) low band.

kurtosis moment delivered oscillating trend, but again with distinct peaks at 0.037 and 0.053 m/s. These peaks in kurtosis indicate that the pressure signal has a distinct distribution in the transition region that distinguish it form the other regimes.

3.2.2. Spectral analysis

We shift our attention to the spectral analysis of the differential pressure signal. It should be noted that very interesting results were observed using this technique. First we examine the spectrum of the pressure signal using the entire record without averaging or dividing the record into smaller segments. The power spectral density (PSD) at various gas velocities is shown in Fig. 7. The curves indicate that the signal carry only low frequency which may be resulted from the oscillation of macrostructure [1]. The low-frequency component is not clear because a large scale is used in the plot. The large scale of the *x*-axes is employed to prove that no high frequency is detected. To fairly compare the effect of gas velocity, the average frequency, f_m is calculated using Eq. (1) and is plotted in Fig. 8. Fig. 8a demonstrates the average frequency over 0–3 kHz bandwidth while Fig. 8b shows the average frequency over 0–200 Hz. The latter is employed to focus on the low-frequency band. Both curves indicate that the pressure fluctuation frequency is slightly high at low gas velocity and then drop to a minimum value around 8 and 4 Hz, respectively. Notice the distinct peak that occurs at critical velocity of 0.037 m/s for both cases.

Alternatively, Figs. 9 and 10 illustrate the results of the spectral analysis when the pressure signals are divided into segments of 512 points with 10% overlapping. This time, the PSD curves reveal the existence of high-frequency components around 900, 1800 and 2500 Hz. Frequency higher than 3000 Hz was also detected but that was purely noise. Note that the high-frequency band disappears starting from 0.058 m/s. The latter value has been found previously in Figs. 5 and 6 to present a critical point. It should be mentioned that this high-frequency band was not observed in the literature because the sampling frequency used in the literature ranges from 50 to 200 Hz. Fig. 10 compares the pressure oscillation frequency at different gas velocity. It appears that the pressure fluctuation decreases gradually as it moves from the bubbly flow regime, which is dominated by

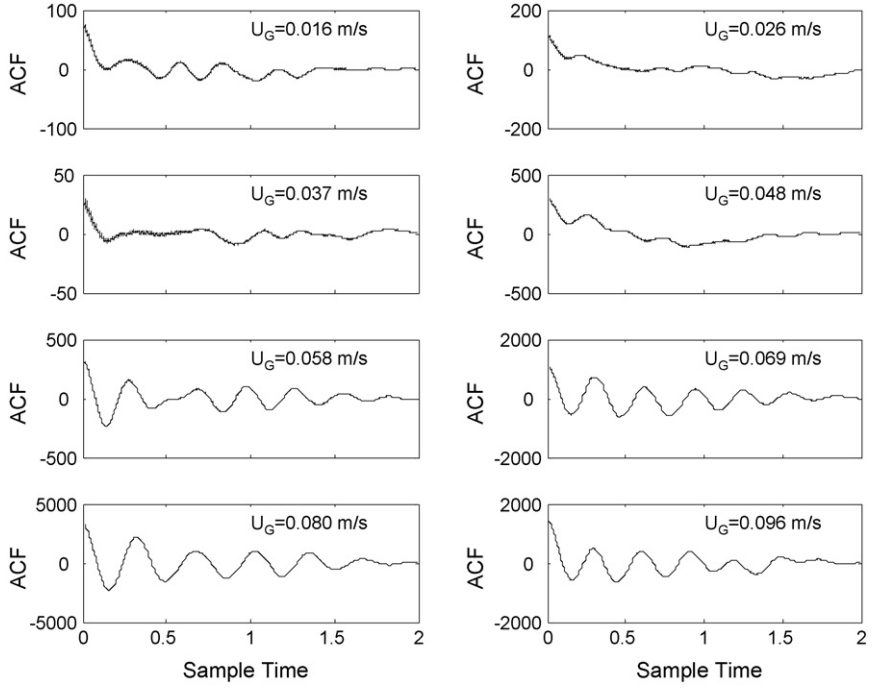

Fig. 13. Auto-correlation function of the differential pressure based on the raw data.

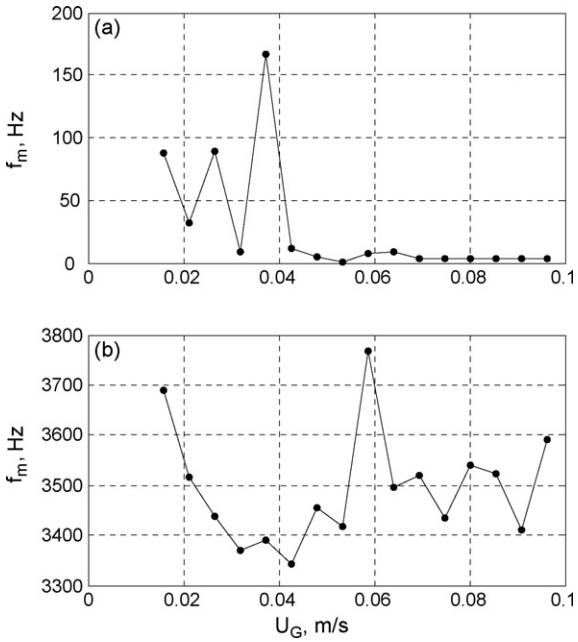

Fig. 14. Average frequency of the auto-correlation in Fig. 13; (a) raw data and (b) differenced data.

high frequency, to a macro-scale liquid circulation manifested by low frequency. The peak at 0.037 m/s appears again in the low-bandwidth-averaged frequency curve. The low frequency of the liquid circulation is found from Fig. 10 to be around 320 and 20 Hz, respectively. This value is much higher than those detected in Fig. 8 and the true value as will be discussed later.

Figs. 11 and 12 depict the spectral analysis results when only a segment of 512 points length of the pressure signal is used. Depending on the sampling frequency, the segment length is shorter than half of the liquid circulation period. Fig. 11 clearly demonstrates the complexity of the flow dynamics across the transitions. In fact, the figure shows how the PSD changes from high-frequency dominant to low-frequency dominant as the gas velocity varies. Obviously, the PSD curve is dominated by high-frequency band at low gas velocity up to 0.053 m/s. This region contains two interesting points one at $U_G = 0.016$ m/s and another at $U_G = 0.037$ m/s. At the first point, i.e., $U_G = 0.016$ m/s, the power strength of the low-frequency component is significant compared to that for high-frequency components. This behavior makes the average frequency, f_m at that point slightly smaller than the next following points as shown in Fig. 12a. Similarly, although the PSD distribution at $U_G = 0.037$ m/s is rich of high-frequency peaks, the low-frequency peak is dominant which in turn reduces the average frequency. The reduction in f_m is marked by sudden drop as shown in Fig. 12a.

At gas velocity of 0.053 m/s, the high-frequency component diminishes compared to the low-frequency component, but the high frequency appears again at U_G of 0.058 m/s. This phenomenon is marked by sudden decrease followed by abrupt increase in the profile of f_m in Fig. 12a. This also explains why these points have special features in the statistical plots shown in Fig. 6. At gas velocities of 0.064 and 0.069 m/s, the high-frequency peaks disappear and recur again at 0.074 m/s. The variation is the PSD is reflected on the average frequency trend shown in Fig. 12a. These observations influence the averaged frequency shown in Fig. 12b too. For example, minimum

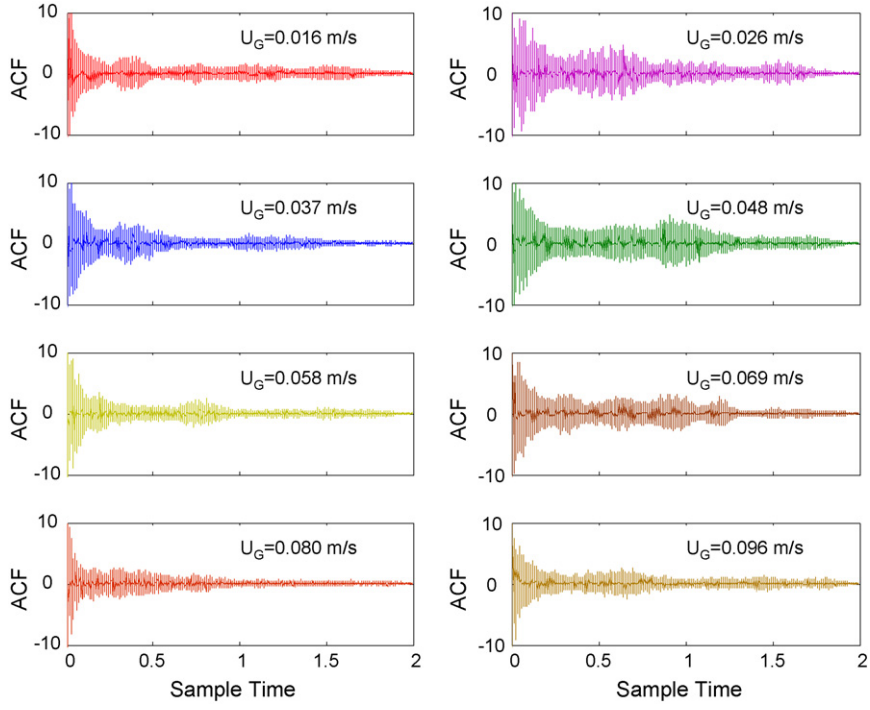

Fig. 15. Auto-correlation function of the differential pressure based on differenced data.

values are observed at 0.037, 0.053 and 0.074 m/s and a pronounced peak at 0.058 m/s. One can argue that these critical values may distinguish more than two flow regimes. In this case, at gas velocity of 0.037 m/s, the homogeneous regime ends followed by the transition region which may end at 0.053 m/s. The point 0.058 m/s may mark the beginning of heterogeneous regime followed by extreme turbulent regime that starts at 0.074 m/s.

The average frequency in Fig. 12b points out that the frequency of the macro-structure is around 50 Hz. Once again this value is incorrect. To rigorously compute the low-frequency oscillation, auto-correlation of the pressure signals is computed and presented in Fig. 13. The auto-correlation function (ACF) is applied to the full record of the raw data to extract the major oscillation in the signal. The ACF curves shown in Fig. 13 do not capture the high-frequency oscillation because it is overshadowed by the prevailing low-frequency oscillation. The smooth and visible fluctuation of the ACF curves facilitates the computation of the oscillation period. Using the method of zero crossing count [3], the period and hence the frequency of each ACF curve in Fig. 13 is computed and plotted in Fig. 14a. Obviously, the mean frequency alternate in the homogeneous regime with a marked peak at 0.037 m/s. Afterward, especially in the heterogeneous regime, the frequency of the pressure fluctuation settles around a constant low value of 3 Hz. This is the frequency of the bubble-induced macro-structures which matches very well the reported value in the literature [1].

In order to capture the high-frequency dynamics, the ACF of the differenced signal is utilized. Data differencing remove the low-frequency component and maintain the high-frequency elements. The ACF curves in Fig. 15 confirm this argument. The existence of multiple high-frequency bands is visible. However, the source and origin of these constituent is not known. The idea is to look at the average frequency in the high bandwidth. The average frequency is shown in Fig. 14b. The average frequency shows a small peak at 0.037 m/s and a paramount peak at 0.058 m/s. We can conclude that the peak at 0.037 m/s comes from the contribution of the low-frequency oscillation while the peak at 0.058 m/s is the outcome of the high-frequency oscillation.

4. Conclusions

In this paper**,** the flow regimes and their transition points in a bubble columns is studied. The phenomenon is investigated through analyzing the acoustic sound signal measured by hydrophone and differential pressure signals measured by pressure transducer. Both statistical moments and spectral density were employed to analyze the signals. Both analysis tools provided interesting qualitative and quantitative information about the flow patterns. Moreover, the transition points predicted from the acoustic signals were consistent with those obtained from the differential pressure signals. The average bubble frequency calculated from the spectrum density of the acoustic signals showed that the critical velocities that mark the end of the homogeneous regime and the start of the heterogeneous regime may occur at 0.037 and 0.066 m/s, respectively. The statistical trends of the acoustic signal involving standard deviation, skewness and kurtosis confirmed the value of the second critical point. However, the first critical velocity predicted by the statistical moments is 0.044 m/s which is slightly higher than that obtained by the spectral analysis.

As far as the differential pressure signals is concerned, application of the statistical moments reconfirm the significance of the gas velocity of 0.037 m/s. This value may be more accurate than 0.044 m/s because it is closer to the value reported in the literature for air–water system which is around 0.03 m/s. Furthermore, the statistical moments and the average frequency obtained from the spectral analysis of the pressure signals signify the gas velocity of 0.058 m/s as the second transition point. The latter values showed interesting structure in the raw, statistical, and spectral trends of the pressure signal. In addition, attractive results are obtained from the way the spectral density is calculated. It is found that the power spectrum of the entire data record does not provide significant information about the flow regimes. The average power spectrum over several segments of the data record showed structural transition from a high-frequency dominant spectrum to a low-frequency dominant spectrum. More relevant information is observed from the power spectrum of a short, but long enough to capture several cycles of the low and high-frequency oscillations, segment of the data record. It is observed that the power spectrum of the pressure signal changes its structure with the gas velocity especially at certain critical values. It should be noted that the auto-correlation function is able to determine the period of the low-frequency oscillation more accurately than the power spectrum.

References

[1] B. Gourich, C. Vial, A. Essadki, F. Allam, M. Soluami, M. Ziyad, Identification of flow regimes and transition points in a bubble column through analysis of differential pressure signal—influence of the coalescence behavior of the liquid phase, Chem. Eng. Process. 45 (2006) 214–223.

[2] J. Zahradnik, M. Fialova, M. Ruzicka, J. Drahos, F. Kastaneck, N. Thomas, Duality of the gas–solid flow regimes in bubble column reactors, Chem. Eng. Sci. 52 (1997) 3811–3826.

[3] W. Al-Masry, E. Ali, Y. Aqeel, Determination of bubble characteristics in bubble columns using statistical analysis of acoustic sound measurements, Chem. Eng. Res. Design 83 (2005) 1196–1207.

[4] T.J. Lin, R.C. Juang, Y.C. Chen, C.C. Chen, Prediction of flow transitions in a bubble columns by chaotic time series analysis of pressure fluctuation signals, Chem. Eng. Sci. 56 (2001) 1057–1065.

[5] W. Al-Masry, E. Ali, Y. Aqeel, Effect of surfactant solutions on bubble characteristics in bubble columns based on acoustic sound measurement, Chem. Eng. Sci. 61 (2006) 3610–3622.

[6] C. Kashev, V. Chilekar, M. Warnier, J. Schaff, B. Kuster, J. Schouten, J. Ommen, Detecting regime transitions in slurry bubble columns using pressure time series, Am. Inst. Chem. Eng. J. 51 (2005) 1951–1965.

[7] V. Chilekar, M. Warnier, J. Schaff, B. Kuster, J. Schouten, J. Ommen, Bubble size estimation in slurry bubble columns from pressure fluctuations, Am. Inst. Chem. Eng. J. 51 (2005) 1924–1937.

[8] C. Vial, E. Camarasa, S. Poncin, G. Wild, N. Midoux, J. Bouillard, Study of hydrodynamic behaviour of bubble columns and external loop airlift reactors through analysis of pressure fluctuations, Chem. Eng. Sci. 55 (2000) 2957–2973.

[9] C. Vial, S. Poncin, G. Wild, N. Midoux, A simple method for regime identification and flow characterization in bubble columns and airlift reactors, Chem. Eng. Sci. 40 (2001) 135–151.

[10] R. Mannasseh, R.F. LaFontain, J. Davy, I.C. Shepherd, Y. Zhu, Passive acoustic bubble sizing in sparged systems, Exp. Fluids 30 (2001) 672–682.
[11] H.M. Letzel, Characterization of regimes and regime transitions in bubble columns by chaos analysis of pressure signals, Chem. Eng. Sci. 52 (1997) 4447–4459.
[12] J. Drahos, F. Bradka, M. Puncochar, Fractal behavior of pressure fluctuations in bubble column, Chem. Eng. Sci. 47 (1992) 4069–4075.
[13] W. Al-Masry, E. Ali, Identification of hydrodynamics characteristics in bubble columns through analysis of acoustic sound measurements—influence of the coalescence behavior of the liquid phase, Chem. Eng. Process. 46 (2007) 127–138.
[14] J. Draho, J. Zahradník, M. Punochá, M. Fialová, F. Bradka, Effect of operating conditions on the characteristics of pressure fluctuations in a bubble column chemical engineering and processing 29 (2) (1991) 107–115.